JOURNAL OF VIROLOGY, May 1999, p. 3595–3602 Vol. 73, No. 5
0022-538X/99/$04.00+0

Retroviral Insertions in *Evi12*, a Novel Common Virus Integration Site Upstream of *Tra1*/*Grp94*, Frequently Coincide with Insertions in the Gene Encoding the Peripheral Cannabinoid Receptor *Cnr2*

PETER J. M. VALK,[1] YOLANDA VANKAN,[1] MARIEKE JOOSTEN,[1] NANCY A. JENKINS,[2] NEAL G. COPELAND,[2] BOB LÖWENBERG,[1] AND RUUD DELWEL[1]*

Institute of Hematology, Erasmus University Rotterdam, 3000 DR, Rotterdam, The Netherlands,[1] and Mammalian Genetics Laboratory, ABL-Basic Research Program, NCI-Frederick Cancer Research and Development Center, Frederick, Maryland 21702[2]

Received 26 October 1998/Accepted 20 January 1999

The common virus integration site (VIS) *Evi11* was recently identified within the gene encoding the hematopoietic G-protein-coupled peripheral cannabinoid receptor *Cnr2* (also referred to as *Cb2*). Here we show that *Cnr2* is a frequent target (12%) for insertion of Cas-Br-M murine leukemia virus (MuLV) in primary tumors in NIH/Swiss mice. Multiple provirus insertions in *Evi11* were cloned and shown to be located within the 3′ untranslated region of the candidate proto-oncogene *Cnr2*. These results suggest that proviral insertion in the *Cnr2* gene is an important step in Cas-Br-M MuLV-induced leukemogenesis in NIH/Swiss mice. To isolate *Evi11*/*Cnr2* collaborating proto-oncogenes, we searched for novel common VISs in the Cas-Br-M MuLV-induced primary tumors and identified a novel frequent common VIS, *Evi12* (14%). Interestingly, 54% of the *Evi11*/*Cnr2*-rearranged primary tumors contained insertions in *Evi12* as well, which suggests cooperative action of the target genes in these two common VISs in leukemogenesis. By interspecific backcross analysis it was shown that *Evi12* resides on mouse chromosome 10 in a region that shares homology with human chromosomes 12q and 19p. Sequence analysis demonstrated that *Evi12* is located upstream of the gene encoding the molecular chaperone *Tra1*/*Grp94*, which was previously mapped to mouse chromosome 10 and human chromosome 12q22–24. Thus, *Tra1*/*Grp94* is a candidate target gene for retroviral activation or inactivation in *Evi12*. However, Northern and Western blot analyses did not provide evidence that proviral insertion had altered the expression of *Tra1*/*Grp94*. Additional studies are required to determine whether *Tra1*/*Grp94* or another candidate proto-oncogene in *Evi12* is involved in leukemogenesis.

During leukemogenesis hematopoietic progenitor cells acquire growth advantages, expand, and accumulate in bone marrow, blood, and other hematopoietic tissues. In this process the expression patterns of multiple critical genes involved in hematopoietic cell proliferation and differentiation change. Human leukemias frequently contain chromosomal translocations (42) and, as a consequence, proto-oncogenes located near these translocations become aberrantly expressed, resulting in the clonal outgrowth of leukemic cells. Retroviral insertional mutagenesis represents an elegant way to study genes involved in hematopoietic tumor formation in mice (21, 55). Retroviral insertion results in activation of proto-oncogenes (2, 22, 35, 36, 40) or inactivation of tumor suppressor genes (7). Multiple human proto-oncogenes and tumor suppressors, e.g., *EVI1* (34), *NF1* (47), and *HOXA9* (39) have been shown to be involved in murine hematopoietic transformation (7, 35, 40) as well, which shows that retroviral insertional mutagenesis in mice clearly shares common features with tumorigenesis in humans. It has generally been accepted that tumor initiation and progression is a multistep process (1, 18, 53). The latency period of several months between retroviral infection and manifestation of the disease suggests that multiple integrations representing mutations in various critical genes may be necessary for complete transformation (21). The cooperation of tumor-inducing genes in leukemia progression has convincingly been demonstrated in proto-oncogene-bearing transgenic mice, which develop tumors more rapidly after retroviral infection than do virus-infected control littermates (1, 5). Thus, the collaboration of various mutated genes can be explored in mouse models by using retroviral insertional mutagenesis. The coexistence of two common virus integration sites (VISs) in multiple tumors may provide an indication for the cooperation of the target genes in malignant transformation (11, 21).

Recently, we identified a novel common VIS, *Evi11*, which is located on mouse chromosome 4 in a region that shares homology with human chromosome 1p36 (51). The common VIS *Evi11* was initially identified in two retrovirally induced myeloid cell lines, NFS107 and NFS78. Subsequently, retroviral insertions in *Evi11* were also demonstrated in multiple primary tumors (51). The cell lines as well as the primary tumors originated from NIH/Swiss mice after inoculation with Cas-Br-M murine leukemia virus (MuLV) (17, 51). The candidate proto-oncogene in this locus is *Cnr2*, the gene encoding the peripheral cannabinoid receptor (51). We and others have shown that murine *Cnr2* is specifically expressed in spleen, thymus, blood cells, and hematopoietic cell lines (14, 37, 50). An endogenous ligand for Cnr2, anandamide, enhances hematopoietic cell proliferation induced by various growth factors, such as interleukin-3 (IL-3), erythropoietin, and granulocyte and granulocyte-macrophage colony-stimulatory factors, in serum-free medium (50). Together, these results suggest a role

* Corresponding author. Mailing address: Institute of Hematology, Erasmus University Rotterdam, P.O. Box 1738, 3000 DR Rotterdam, The Netherlands. Phone: 31104087843. Fax: 31104362315. E-mail: Delwel@hema.fgg.eur.nl.

for aberrantly expressed Cnr2 receptors in leukemia development.

In this study we investigated the exact location and the frequency of retroviral insertions in *Evi11*/*Cnr2* in a new panel of 91 Cas-Br-M MuLV-induced primary tumors in NIH/Swiss mice and 20 previously established cell lines (17, 19). Retroviral insertion in *Evi11* occurred frequently, i.e., in 13 of 111 cases studied. These proviral integrations in *Evi11* were mainly located in the 3′ untranslated region (UTR) of *Cnr2*. To search for new common VISs and to isolate oncogenes cooperating with *Evi11*/*Cnr2*, new provirus flanking cDNA fragments were isolated from the *Evi11*/*Cnr2*-rearranged myeloid cell line NFS107. We identified a novel frequent common VIS, *Evi12*, which was found in 16 of our panel of 111 primary tumors and cell lines. Proviruses in *Evi12* inserted upstream of the gene encoding the molecular chaperone *Tra1*/*Grp94*. Interestingly, in 54% of the *Evi11*/*Cnr2* rearranged tumors insertions were also observed in *Evi12*, suggesting that the target proto-oncogenes in *Evi11*/*Cnr2* and *Evi12* collaborate in leukemic transformation.

MATERIALS AND METHODS

Cell lines. The myeloid cell line NFS107 was established in vitro from Cas-Br-M MuLV-initiated primary tumors (17). The NFS (17) and DA (19) cell lines were cultured in RPMI 1640 medium supplemented with penicillin (100 IU/ml), streptomycin (100 ng/ml), 10% fetal calf serum, and murine IL-3 (1 μg/ml).

Primary tumors. Newborn NIH/Swiss mice were injected subcutaneously with cell culture supernatant of Cas-Br-M MuLV producing NIH 3T3 cells (obtained from H. Morse III and J. W. Hartley). Between 150 and 220 days after injection the mice developed leukemias. Ninety-one leukemic mice were sacrificed when moribund. Forty-seven leukemic mice had 5- to 10-fold-enlarged spleens, and 17 mice had slightly enlarged spleens (up to 2-fold). Lymph nodes and thymus were isolated when they were enlarged. Cells from spleen, thymus, or lymph nodes from 91 Cas-Br-M MuLV-infected mice (CSL [Cas-Br-M MuLV Swiss leukemia]) were cryopreserved in liquid nitrogen. From these cells, high-molecular-weight DNA was isolated (46) for Southern blot analysis. To analyze the morphology of the primary tumor cells, cells were examined after May-Grünwald-Giemsa staining.

PCRs. To determine the exact locations and orientations of Cas-Br-M provirus in the *Evi11* and *Evi12* loci, PCR was carried out on 1 μg of genomic DNA from the primary tumors with VIS-specific primers in combination with Cas-Br-M MuLV long-terminal-repeat (LTR)-specific primers (Fig. 1A [*Evi11*] and 4A [*Evi12*]). Insertions in *Evi11* were amplified with primer CBR16 (5′-GTATTTC AACATCAACTTGG-3′) and primer pLTR-A (5′-CCGAAACTGCTTACCA C-3′) (cycling conditions were 1 min at 94°C, 1 min at 48°C, and 3 min at 72°C [30 cycles]), followed by nested PCRs with CBR22 (5′-CCTCTCATTGCTCTA ACATG-3′) and pLTR-B (5′-CTGTTTGGCCCAACTTCAGCTG-3′) (cycling conditions were 1 min at 94°C, 1 min at 58°C, and 3 min at 72°C [30 cycles]). To determine virus integrations in *Evi12*, PCR was carried out with primer p503-1 (5′-GTGTGAAAACCCTAATTCCGG-3′) and pLTR1 (5′-GGGTCTCCTCA GAGTGATTG-3′) (cycling conditions were 1 min at 94°C, 1 min at 57°C, and 3 min at 72°C [30 cycles]), followed by PCR with p503-1 and pLTR2 (5′-TAAGT CGACTACCCGCCTCG-3′) (cycling conditions were 1 min at 94°C, 1 min at 48°C, and 3 min at 72°C [30 cycles]). A reverse transcription-PCR (RT-PCR) strategy was carried out to isolate cDNA fragments from NFS107 flanking VISs as described previously (52). Poly(A)$^+$ RNA was purified from NFS107 by affinity chromatography with oligo(dT) cellulose columns (Pharmacia). Reverse transcriptase reactions were performed for 1.5 h at 37°C with 3 μg of poly(A)$^+$ RNA in 50 mM Tris-HCl (pH 8.3), 75 mM KCl, 3 mM $MgCl_2$, 1 mM dithiothreitol, 0.5 mM deoxynucleoside triphosphates (dNTPs), 1 U of RNAguard (Pharmacia), and 100 U of SuperScript RT (Gibco, Breda, The Netherlands). For first-strand synthesis 40 mM oligo(dT) adapter [5′-GTCGCGAATTCGTC-GACGCG(dT)$_{15}$-3′] was used. Subsequently, PCR was carried out by using the adapter primer (5′-GTCGCGAATTCGTCGACGCG-3′) in combination with the LTR-specific primer pLTR1 (5′-GGGTCTCCTCAGAGTGATTG-3′) to isolate the cDNA fragments adjacent to the VISs. The PCR reaction mixture contained 10 mM Tris-HCl (pH 8.3), 50 mM KCl, 1.5 mM $MgCl_2$, 150 μM dNTPs, and 2.5 U of *Taq* polymerase (Pharmacia, Uppsala, Sweden). Reactions started with 10 min at 94°C and ended with 10 min at 72°C. Products were cloned into pBluescript II SK(+) (*Eco*RV) (Statagene, Westburg, Leusden, The Netherlands) and sequenced.

Sequence analysis. Nucleotide sequencing was performed on the ABI 310 sequencer (Perkin-Elmer, Nieuwerkerk, The Netherlands). Fragments were cloned into pBluescript II SK(+) and sequenced with T_3, T_7, or sequence-specific primers. Deduced sequences were analyzed by using the BLAST network service of the National Center for Biotechnology Information (NCBI).

Southern and Northern blot analysis. Southern and Northern blot analysis were performed as described previously (51).

Interspecific backcross mapping. Interspecific backcross progeny were generated by mating (C57BL/6J × *Mus spretus*)F_1 females and C57BL/6J males as described previously (10). A total of 205 N_2 backcross mice were used to map the *Evi12* locus (see Results for details). DNA isolation, restriction enzyme digestion, agarose gel electrophoresis, Southern blot transfer, and hybridization were performed essentially as described earlier (20). All blots were prepared with Hybond-N$^+$ nylon membrane (Amersham). The 503 probe, a 233-bp cDNA fragment flanking a VIS in NFS107, was labelled with [α-^{32}P]dCTP by using a random prime labelling kit (Stratagene); washing was done to a final stringency of 1.0× SSCP (0.12 M NaCl plus 15 mM $Na_3C_6H_5O_7$ and 20 mM $NaPO_4$)–0.1% sodium dodecyl sulfate at 65°C. A 5.5-kb fragment was detected in *Hin*dIII-digested C57BL/6J DNA, and a fragment of 4.3 kb was detected in *Hin*dIII-digested *M. spretus* DNA. The presence or absence of the 4.3-kb *Hin*dIII *M. spretus*-specific fragment was monitored in backcross mice.

A description of the probes and the restriction fragment length polymorphisms (RFLPs) for the loci linked to the *Evi12* locus, including *Gna15*, *Pah* and *Tmpo*, been reported previously (3, 54). Recombination distances were calculated by using Map Manager, version 2.6.5. The gene order was determined by minimizing the number of recombination events required to explain the allele distribution patterns.

Western blot analysis. NFS cells were washed with ice-cold phosphate-buffered saline with 10 mM Na_3VO_4. Subsequently, cells were spun down and lysed by incubation for 10 min at 4°C in lysis buffer (50 mM Tris-HCl, pH 8.0; 100 mM NaCl; 1% Triton X-100; 0.1 mM Na_3VO_4; 1% Pefabloc SC; 50 μg of aprotinin, 50 μg of leupeptin, 50 μg of bacitracin, and 50 μg of iodoacetamide per ml; and 1 mM dithiothreitol). Insoluble material was removed by centrifugation for 30 min at 10,000 × *g* at 4°C. After sodium dodecyl sulfate-polyacrylamide gel electrophoresis, proteins were electroblotted onto nitrocellulose (0.2 μm; Schleicher & Schuell, Dassel, Germany). Filters were blocked by incubation in 0.3% Tween 20 in Tris-buffered saline (TBS; 10 mM Tris-HCl, pH 7.4; 150 mM NaCl) for 1 h at 37°C, washed in TBST (0.05% Tween 20 in TBS), and incubated with antibodies diluted in TBST. The Grp94 antibody used for Western blotting was goat polyclonal anti-Grp94 (Santa Cruz Biotechnology, Inc., Santa Cruz, Calif.). After being washed with TBST, immune complexes were detected with horseradish peroxidase-conjugated anti-goat immunoglobulin Gspecific antiserum (Santa Cruz Biotechnology), followed by an enhanced chemiluminescence reaction (DuPont, Boston, Mass.).

Nucleotide sequence accession number. The accession number for the 1.7-kb fragment containing the Cas-Br-M MuLV insertion sites is AF091114.

RESULTS

Frequent retroviral insertions in the *Cnr2* gene in *Evi11*. Recently, we demonstrated that retroviral insertions in the *Evi11* locus in two Cas-Br-M MuLV-induced cell lines, NFS78 and NFS107, and in five Cas-Br-M MuLV-induced primary tumors occurred in the *Cnr2* gene (51). To determine the frequency of retroviral insertions in *Evi11*, we screened DNA from a panel of 111 leukemias, i.e., 91 Cas-Br-M MuLV-induced tumors and 20 cell lines (17, 19) by Southern blot analysis with a probe complementary to the protein-coding region of *Cnr2* (probe C, Fig. 1A) (reference 51 and data not shown). Rearrangements in *Evi11*/*Cnr2* were found in 13 of 111 cases (12%; Table 1). Based on the restriction enzyme map of Cas-Br-M MuLV (accession number X57540) and the restriction sites within the *Evi11*/*Cnr2* locus (51), the orientations of the retroviruses were determined (Fig. 1A). In all primary tumors provirus integrations occurred in the same orientation, i.e., in the direction of transcription of the *Cnr2* gene. After PCR (Fig. 1A) with the LTR-specific primers pLTR-A and pLTR-B in combination with the *Cnr2*-specific primers CBR16 and CBR22, respectively, the exact sites of proviral insertion in a number of primary tumors were determined (Fig. 1B). As shown in Fig. 1B, all proviruses, except CSL75, were located in the 3′ UTR of the *Cnr2* gene. Based on Southern blot analysis, it was concluded that as a result of recombination the genomic structure of the *Evi11* locus in CSL63 was altered (data not shown). How retroviral insertion affects expression of Cnr2 receptors in the *Cnr2*-mutated leukemias is the subject of current investigations. In this study we focus on the identification of novel common VISs representing transforming genes cooperating with *Cnr2* in leukemogenesis.

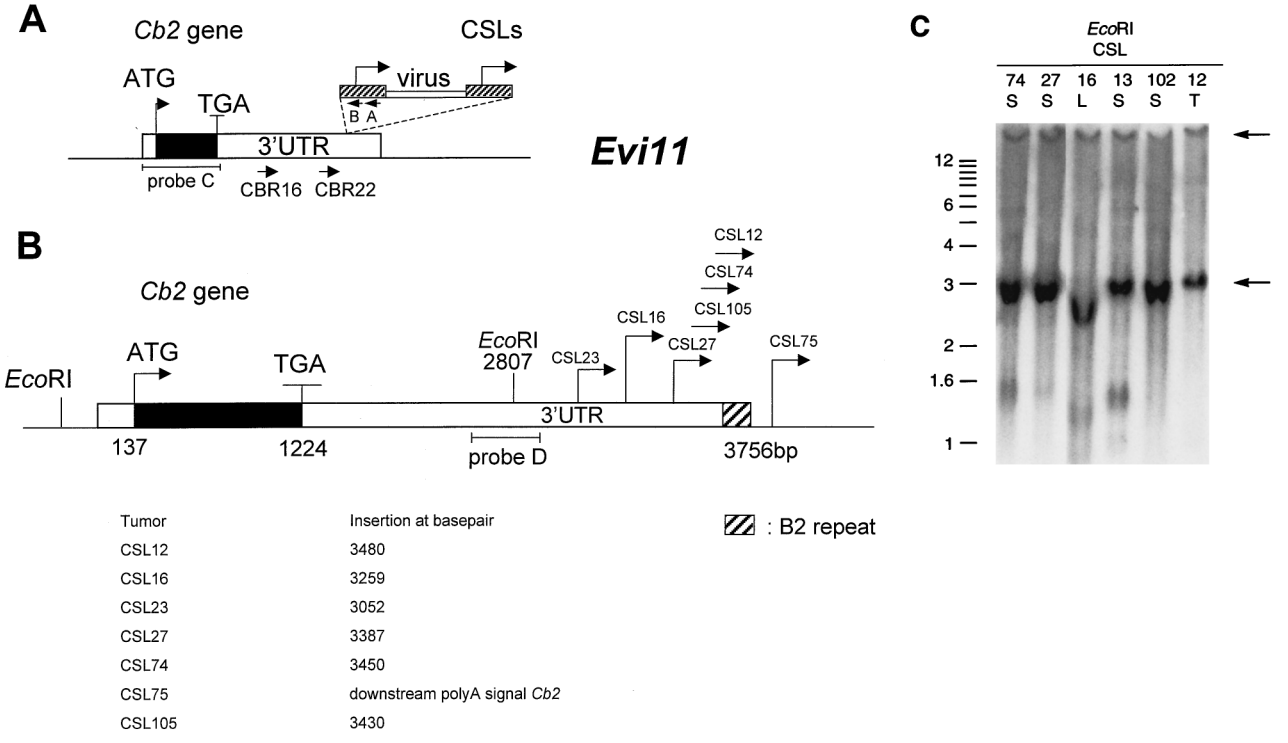

Tumor	Insertion at basepair
CSL12	3480
CSL16	3259
CSL23	3052
CSL27	3387
CSL74	3450
CSL75	downstream polyA signal *Cb2*
CSL105	3430

▨ : B2 repeat

FIG. 1. Isolation of Cas-Br-M MuLV proviral insertions in *Evi11/Cnr2*. (A) Schematic representation of the *Cnr2* gene in the *Evi11* locus and the orientation and site of integration of proviral DNA within the 3′ UTR of *Cnr2* in the primary tumors (CSLs). The locations of the primers used for PCR amplification on genomic DNA, i.e., primers set CBR16 and pLTR-A followed by CBR22 and pLTR-B are indicated by small arrows. Probe C used for Southern blot analysis of the primary tumors (data not shown and reference 51) is indicated. The protein-coding region of the *Cnr2* gene is indicated by the black box. (B) Exact locations of the proviral integrations in various independent Cas-Br-M MuLV-induced primary tumors in the 3′ UTR of the *Cnr2* gene. An arrow with a CSL number indicates the insertion site in this particular tumor. Probe D was used for Southern blot analysis (Fig. 1C). The protein-coding region of the *Cnr2* gene is indicated by the black box. (C) Southern blot analysis of high-molecular-weight DNA of Cas-Br-M MuLV-induced primary tumors digested with *Eco*RI to detect MCF viruses. Hybridizations were performed with probe D (*Hin*dIII/*Nco*I fragment [at bp 2,474 and 2,974 of the *Cnr2* cDNA, respectively) (Fig. 1B) (51). Since this probe contains an *Eco*RI site, two bands representing a normal allele appear indicated by arrows. Rearranged fragments of approximately 1.6 kb were detected in CSL13, CSL16, CSL27, and CSL74 but not in the control tumors CSL102 and CSL12 without rearrangements in *Evi11/Cnr2* (S, spleen; T, thymus; L, lymph nodes). The rearranged fragments represent the leukemic cell population containing provirus in *Evi11/Cnr2*.

Identification of a novel common virus integration site, *Evi12*. To isolate *Evi11/Cnr2* cooperating transforming genes, we applied a novel RT-PCR technique (52) on RNA from NFS107, a retrovirally induced myeloid tumor cell line with a provirus insertion in *Evi11/Cnr2* (51). Multiple novel cDNA fragments flanking provirus were isolated from NFS107 (data not shown). A cDNA fragment of 233 bp, designated 503, was cloned into pBluescript SK(+) and sequenced (see Fig. 4B). No homologous sequences were found by searching the database of the NCBI. RT-PCR analysis with primer set 503-2 (see Fig. 4B) and pLTR1 demonstrated high mRNA expression of cDNA fragment 503 in NFS107 compared to control cell lines. It is at present uncertain whether cDNA fragment 503 represents a transcript of a cellular gene (52), since no mRNA was detected in RNA from various murine tissues by using Northern blot analysis or RNase protection analysis (data not shown). However, Southern blot analysis with 503 on high-molecular-weight DNA from all 91 Cas-Br-M MuLV-induced primary tumors demonstrated rearranged alleles in a number of independent tumors, e.g., CSL17, CSL27, CSL29, CSL85, CSL89, CSL93, and CSL97 (Fig. 2). From Southern blot analyses of the primary tumors digested with multiple enzymes and the restriction enzyme map of Cas-Br-M MuLV (accession number X57540), it was concluded that the DNA rearrangements were indeed the result of proviral integration (data not shown). To date, we have identified rearrangements in this locus in 15 of 91 primary tumors, and we have designated this ecotropic virus integration site 12 or *Evi12*. From the 20 cell lines studied so far, an *Evi12* rearrangement was shown in one cell line, i.e., NFS107.

Insertion of mink cell focus-forming (MCF) viruses in *Evi11/Cnr2* and *Evi12*. The primary tumors were isolated from the outbred NIH/Swiss mice that were infected with ecotropic Cas-Br-M MuLV (15, 25). Inoculation of NFS/N and NIH/Swiss mice with Cas-Br-M MuLV results in the production of both ecotropic and MCF recombinant MuLVs (16, 25). Most of the MCF MuLVs are identified by a unique *Eco*RI site within the *env* gene in the proviral genome (44). Interestingly, based on the size of the rearranged alleles after *Eco*RI digestion in *Evi11/Cnr2*-rearranged tumors (ca. 1.6 kb; Fig. 1C), an *Eco*RI site must be located just downstream of the 5′ LTR. The size of the rearranged alleles after *Eco*RI digestion in *Evi12*-rearranged tumors (ca. 2.0 kb; Fig. 2) is indicative for the MCF virus unique *Eco*RI site at 6.9 kb of the proviral genome (44). Southern blot analysis demonstrated that in the Cas-Br-M MuLV-induced primary tumors, all proviruses in either *Evi11/Cnr2* or *Evi12* are of the MCF type (Table 1).

***Evi12* is located on the central region of mouse chromosome 10.** The mouse chromosomal location of *Evi12* was determined by interspecific backcross analysis by using progeny derived

TABLE 1. *Evi11* and *Evi12* insertions in Cas-Br-M MuLV-induced CSL primary tumors in NIH/Swiss mice[a]

Tumor number	Tissue type	Phenotype	Latency period (days)	*Evi11*	*Evi12*
CSL11	Spleen	ND	137		M
CSL12	Spleen and thymus	ND	148	PCR	M
CSL13	Spleen	ND †	166	M	M
CSL14	Thymus and spleen	ND	167	M	M
CSL15	Spleen	ND †	170		M
CSL16	Lymph node	Lymphoid	196	M	M
CSL17	Thymus	Lymphoid	175		M
CSL23	Spleen	ND	203	PCR	
CSL27	Thymus and spleen	Immature blasts	191	M	M
CSL29	Spleen	ND †	208		M
CSL35	Spleen	Immature blasts	196		M
CSL60	Spleen	Immature blasts	224		M
CSL63	Thymus	Lymphoid	209	M [R]	
CSL74	Spleen	ND	216	M	
CSL75	Spleen	ND	216	M	
CSL85	Spleen	Immature blasts	210		M
CSL89	Lymph node and spleen	Immature blasts	229		M
CSL93	Spleen	ND †	229		M
CSL97	Spleen	ND †	253	M	M
CSL105	Spleen	Immature blasts	294	M	
NFS78	Cell line	Myeloid		E	
NFS107	Cell line	Myeloid		M	E

[a] Abbreviations (phenotypes were determined by morphology after May-Grünwald staining): M, MCF MuLV; E, ecotropic MuLV; [R], unable to determine exact MuLV insertion in the *Cb2* gene because of recombination of the *Evi11*/*Cb2* locus; ND, not determined; PCR, rearrangement undetectable by Southern blot analysis, proviral insertion determined by PCR (Fig. 1B). A dagger indicates the mice were dead.

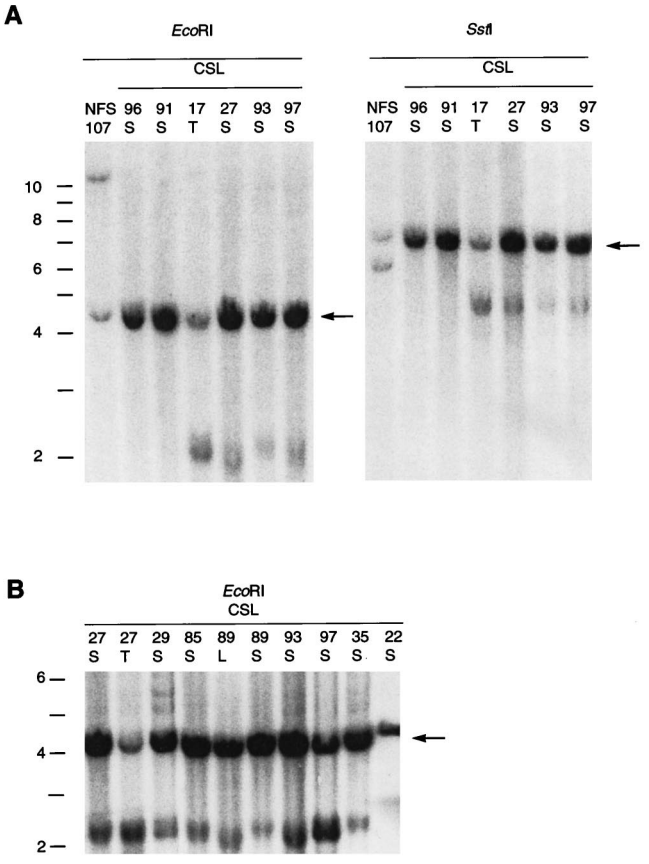

FIG. 2. Identification of common virus integration site Evi12. Southern blot analysis of high-molecular-weight DNA of NFS107 and a number of Cas-Br-M MuLV-induced primary tumors (CSL) digested with *Eco*RI or *Sst*I. Filters were hybridized with fragment 503 (Fig. 6). Rearrangements (2.0 kb) were detected in CSL17, CSL27, CSL29, CSL85, CSL89, CSL93, and CSL97 but not in with the control tumors CSL22, CSL91, and CSL96 (S, spleen; T, thymus; L, lymph nodes). Arrows indicate the normal nonrearranged alleles.

from matings of ([C57BL/6J × *Mus spretus*]F_1 females × C57BL/6J) mice. This interspecific backcross mapping panel has been typed for over 2,500 loci that are well distributed among all autosomes, as well as the X chromosome (10). C57BL/6J and *M. spretus* DNAs were digested with several enzymes and analyzed by Southern blot hybridization for informative RFLPs by using the 233-bp mouse 503 cDNA probe. The 4.3-kb *Hin*dIII *M. spretus* RFLP (see Materials and Methods) was used to monitor the segregation of the *Evi12* locus in backcross mice. The mapping results indicated that *Evi12* is located in the central region of mouse chromosome 10 linked to *Gna15*, *Pah*, and *Tmpo*. Although 126 mice were analyzed for every marker and are shown in the segregation analysis (Fig. 3), up to 177 mice were typed for some pairs of markers. Each locus was analyzed in pairwise combinations for recombination frequencies with the additional data. The ratios of the total number of mice exhibiting recombinant chromosomes to the total number of mice analyzed for each pair of loci and the most likely gene order are as follows: centromere - *Gna15* - 7/139 - *Evi12* - 1/137 - *Pah* - 5/177 - *Tmpo*. The recombination frequencies (expressed as genetic distances in centiMorgans [cM] ± the standard error) are as follows: - *Gna15* - 5.0 ± 1.9 - *Evi12* - 0.7 ± 0.7 - *Pah* - 2.8 ± 1.3 - *Tmpo*. We have compared our interspecific backcross map of chromosome 10 with a composite mouse linkage map that reports the map location of many uncloned mouse mutations (provided from The Mouse Genome Database, a computerized database maintained at The Jackson Laboratory, Bar Harbor, Maine). *Evi12* mapped in a region of the composite map that lacks mouse mutations with a phenotype that might be expected for an alteration in this locus (data not shown). The central region of mouse chromosome 10 shares regions of homology with human chromosomes 19p and 12q (summarized in Fig. 3), suggesting that the human homolog of *Evi12* will map to 19p or 12q.

***Evi12* is located near the promoter region of the *Tra1*/*Grp94* gene.** Following a PCR approach (Fig. 4A), we have cloned the MuLV integration sites in *Evi12* from 13 primary tumors (Fig. 4B). These *Evi12* proviral insertions were located within a region of approximately 1.7 kb and had been inserted opposite to the proviral integration in NFS107 (Fig. 4B and 5). The nucleotide sequence of the 1.7-kb PCR fragment from CSL16 was compared with sequences in the NCBI database and demonstrated high homology with the promoter region of the *Sus scrofa Ppk98* gene (X90848) (Fig. 4B) (12, 13). The murine homolog of porcine *Ppk98* is *Tra1*/*Grp94* (also referred to as *Erp99*, endoplasmin, and *Gp96* in other studies). The gene encoding *Tra1*/*Grp94* is located on mouse chromosome 10 (49) in a region that shares homology with human chromosome 12q (28, 45). This suggested that the retroviral integrations in *Evi12* were located upstream of the murine *Tra1*/*Grp94* gene. The 233-bp fragment 503 was, subsequently, used to screen an embryonic stem cell (E14) mouse genomic library to isolate genomic DNA fragments representing the *Evi12* locus. One phage clone (λ503) was isolated and used to generate a restriction enzyme map (Fig. 5). This map showed identity with the 5′ region of the mouse *Tra1*/*Grp94* gene (48), which confirmed that *Evi12* is indeed located upstream of the gene encoding the

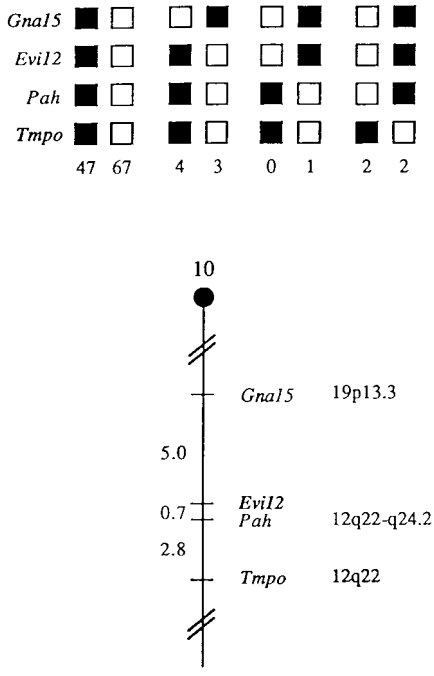

FIG. 3. *Evi12* maps in the central region of mouse chromosome 10. *Evi12* was placed on mouse chromosome 10 by interspecific backcross analysis. The segregation patterns of *Evi12* and flanking genes in 126 backcross animals that were typed for all loci are shown at the top of the figure. For individual pairs of loci, more than 126 animals were typed (see text). Each column represents the chromosome identified in the backcross progeny that was inherited from the (C57BL/6J × *M. spretus*)F_1 parent. The shaded boxes represent the presence of a C57BL/6J allele, and the white boxes represent the presence of a *M. spretus* allele. The number of offspring inheriting each type of chromosome is listed at the bottom of each column. A partial chromosome 10 linkage map showing the location of *Evi12* in relation to linked genes is shown at the bottom of the figure. Recombination distances between loci in centiMorgans (cM) are shown to the left of the chromosome, and the positions of loci in human chromosomes are shown to the right. References for human map positions can be obtained from the GDB (Genome Data Base), a computerized database of human linkage information maintained by The William H. Welch Medical Library of The Johns Hopkins University (Baltimore, Md.).

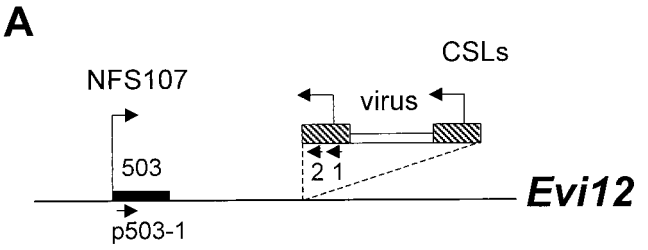

B

```
>NFS107
1    ATGTGAGTGT GAAAACCCTA ATTCCGGTTA TAGTTCAAGT GGGGCAATCA TTTTATCCAC
     p503-1
61   TAAGCCATCT CTCCTCAGCT GAAAGCATGT ATTTTCCAGG AGCTTGGCCA GCAAGTCAAG
121  ATAAGGACTG ACCATCTTCT GCCAGCCTGG AAGTAGATTC TCTCTCTCTG ATTCTCTCTC
     <CSL15
181  TCTCTCCTTT CTATCTGGGG ACCATCATCT GCAGAAACTT CTACCCCCCC CCCAAAAAAA
                                              p503-2
241  AAAAAAAAAA AGAACAAAAC CAAAAACCCA CCAGCTTTAT TTTGGAGGAC AAATCTCATT
                    <CSL29
               <CSL85
301  CTCAGTTCCT CCCAGGTGCA GCCCGATCTA CCTCCCACTG GCCAGTTAAG ATGCAGTCAC
361  AGTTTCACAA TACTTGCTTA CTTGCTCGAT AAAAAAAAAA AGAAAGGAAG AAAGAAAGAA
                    <CSL17                <CSL14
421  AGAAAGAAAG AAAGAAAGAA AGAAAGAGAG TAAGAAAGAA AGAAAGTGGA TGATGGGCTG
          <CSL97
     <CSL89                                                        <
481  TCATACGCAG AAATGGCCAT CTTTTTCCAA AAGCACAAAT AAATAAGATC CTGGTATGCT
     CSL12S
541  CTAAACAACA AACACAAGCA CAGAGGCATA AGGCCTTCGT CTTACATTTC TGTATGCTTT
                                        <CSL60
                                  <CSL11          <CSL35
601  GGCAAATGTA GGTAAATCAG ACAGATGTAA ATAAGCCATC ACCACATTAT GTAAACACCA
661  AACCACAGAT TCAAGTTCTA CAAGTCTAAA TTCTTGAAGT GTCAAAGGGA CTATGACATT
                                              <CSL13
721  GTCACTGAAA AGCTTGCCTT CGAGAACCTG GATTGCCTAA AAAAAAACAT CTCGAATTTT
          <CSL12T
781  CTTGGAGAAA GCGGTGATGG AATGGATGTG TTGAGGGCAG GCAAGCGTGC TGGTGGAAAA
841  TTGGTTAAAA TGAGGCTAAA GAGCCTAGAA AACATTTCGG AACGTACAAG CTGGCCCTAG
901  GGACTTCCCT CACCAGAAAG AGCCTCTTTT GCTATCTTTC GGAAGGCGGA AAGGTGTTTC
961  TATGAAGTTA CAAAGCCACA ATCCAGGCTG TTTTGCAAGC TCTGCGGCTT TTGCTTTCAA
1021 GTATCTGCAT AAGTTCTTTC CTGTTCTATG CTAGCCTGGA CTTCACCACC GCGCTCTCTG
1081 GCTGATTCAC AAAAGAGGCT CTAGATTGCC CAGTCATTCT TTGATATTTA TGGGGATGTC
1141 AAAGGAACTT GGGTCCTTGT TTCCTTCGGG GTTGGAGAGC CCCTACATCC TCAACTGCAA
1201 ACCAAACCAG AGAGGACAGG AAATGCGAGC AGCGCAACGC CAAGTGTAAC CGAAGGCTCT
1261 AGGGACCCTG AGTGACGCGC AAGAAAGCGG ACGTGGAAAC CCGGGTGCTA CCACCAGCCC
1321 AGAATCCAGG GCTGACCCTC TGACACGGTG AGACTAGGGC TACGCGGGGC TGCTTTTCAG
1381 GTCCGCCTCT GAAAACTGTG TGCATTAGAG TCCTAGAACA AGCACAGATC TATTCTGCAA
1441 TCTGAATGAG GTGGNAATCC TATAATCACT CAGAGACATT TCCCGCGGAC ACAAGATTGG
1501 AGTAAGCAAG GGCCAAGTAC GCAACTGGCC TAGACGCCAG AGACTACAAT TCCCAGCATT
1561 CATGAGATTA GTGCGTTGCA TGCCGGAAAC TGTAGTTTCT CACCACCATC CAAACGCATT
1621 CCGGATATTC AACCCCTCAC AAATTTCTCT TTTGCGAAAA GAAACGCCCA AAAGAAAGGT
1681 GACGGCGAAC GTAGCGCTGA AAGGACTCGT AACGTGACCC GCGTCGTAGA CGAGAAAAGG
     <CSL16
1741 GT
```

FIG. 4. Locations of proviral insertions in the *Evi12* locus. (A) Representation of the proviral integration in *Evi12* in the myeloid cell line NFS107. Fragment 503 flanking provirus in NFS107 and the orientation and site of insertion of the proviruses in the primary tumors (CSLs) are shown. VISs were amplified with primer set p503-1 and pLTR1 followed by p503-1 and pLTR2. (B) DNA sequence of the 1.7-kb region and the locations and orientations of the retroviral integrations in *Evi12* identified in the myeloid cell line NFS107 and the Cas-Br-M MuLV-induced primary tumors (CSL). The first 233 bp represent fragment 503. Both 503-specific primers, p503-1 and p503-2, are indicated by an arrow. cDNA synthesis of fragment 503 was primed on the poly(A) stretch from 234 to 276 bp. The region homologous to the promoter of the *S. scrofa ppk98* gene (NCBI; E value, 1.10^{-6}) is double underlined.

molecular chaperone, *Tra1/Grp94* (Fig. 5). Moreover, sequence analysis demonstrated coding sequences of *Tra1/Grp94* on a 1.6-kb *Eco*RI fragment isolated from λ503 (Fig. 5). Although *Tra1/Grp94* is constitutively expressed in the endoplasmic reticulum (ER) of all eukaryotic cells (30), we investigated whether expression of this gene was altered in the myeloid cell line NFS107 and the primary tumors CSL11 and CSL17, which contain provirus in *Evi12*. Northern blot analysis demonstrated comparable levels of *Tra1/Grp94* mRNA in NFS107 and in cell lines without retroviral insertions in *Evi12*, i.e., DA3, NFS22, NFS60, NFS61, and NFS70 (Fig. 6A). Likewise, no changes in *Tra1/Grp94* mRNA expression were observed in CSL11 and CSL17 (Fig. 6A). Moreover, no fusion or readthrough mRNA transcripts of retroviral sequences and *Tra1/Grp94* were apparent by Northern blot analysis. Western blot analysis showed comparable *Tra1/Grp94* protein levels in NFS107 and control cell lines without *Evi12* insertions, i.e., NFS22, NFS61, NFS70, and NFS78 (Fig. 6B). Recent studies showed that expression of *Tra1/Grp94* and the ER molecular chaperone *Grp78* is tightly regulated by hematopoietic growth factors (6). Although we were able to reproduce the results of Brewer and coworkers, i.e., induction of *Tra1/Grp94* mRNA expression by IL-3 in growth-factor-deprived cell lines, no differences were observed between NFS107 (*Evi12* provirus insertion) and DA3 (no *Evi12* provirus insertion) (data not shown). Together, these results indicated that *Grp94* is located near the common VIS *Evi12* but that expression of the *Tra1/Grp94* gene is not affected as a result of proviral insertion in *Evi12*.

High coincidence of retroviral insertion in *Evi11* and *Evi12* in Cas-Br-M MuLV-induced primary tumors. The *Evi12* flank-

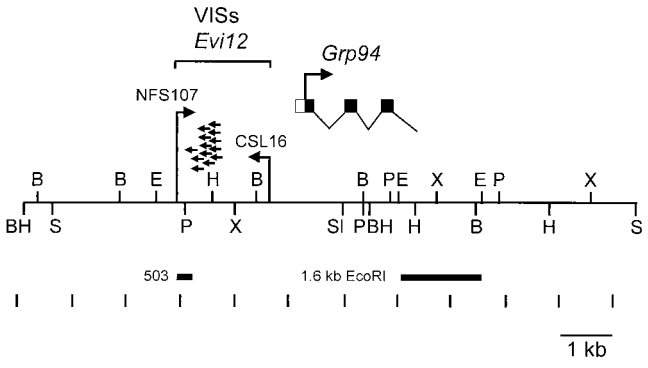

FIG. 5. Restriction enzyme map of the *Evi12* locus. Restriction map of the genomic phage λ503 representing the *Evi12* locus (Sl, *Sal*I; S, *Sst*I; BH, *Bam*HI; P, *Pst*I; B, *Bgl*II; H, *Hin*dIII; X, *Xba*I; E, *Eco*RI). The proviral insertion region of 1.7 kb is flanked by the virus integration sites in NFS107 and CSL16. Arrows indicate the viral insertions in the other CSL tumors. The locations of the first three exons of the *Tra1*/*Grp94* gene are depicted as boxes, with the protein-coding region in black. The 1.6-kb *Eco*RI fragment used for sequence analysis and the cDNA fragment 503 flanking the *Evi12* VIS in NFS107 are indicated below the restriction map.

ing cDNA 503 was isolated from the IL-3-dependent myeloid cell line NFS107 that also contains an insertion in *Evi11*/*Cnr2*. In fact, 54% of the tumors, i.e., 7 of 13, bearing provirus within *Evi11*/*Cnr2* contained insertions in the novel common VIS *Evi12* as well (Table 1). The equal intensities of the rearrangements in *Evi11* or *Evi12* in each tumor containing insertions in both these loci shown by Southern blot analysis suggest a clonal outgrowth of leukemic cells (data not shown). The high percentage of coincidence between *Evi11* and *Evi12* demonstrated in this study provides evidence for cooperative transforming activity between the target proto-oncogenes in *Evi11* and *Evi12*.

DISCUSSION

Tumor initiation and progression is a multistep process (1, 18, 53). Therefore, proviral insertion in *Evi11*/*Cnr2* is probably one of multiple genetic alterations required before a hematopoietic progenitor cell becomes fully malignant. Interestingly, in outbred NIH/Swiss mice, *Evi11*/*Cnr2* is a frequent target for Cas-Br-M MuLV (12%). In an attempt to isolate *Evi11*/*Cnr2* cooperating genes, novel provirus flanking cDNA fragments were isolated (52). Clone 503 represented a novel common VIS *Evi12*, which was found in 14% of the Cas-Br-M MuLV-induced NIH/Swiss leukemias. More interestingly, 54% of the tumors containing proviruses in the gene encoding the peripheral cannabinoid receptor *Cnr2* also have insertions in *Evi12*. Retroviral infection of *Cnr2* transgenic mice (1, 5), with the *Cnr2* gene controlled by the *Sca1* promoter (33), is currently being performed to determine whether transgenic mice develop leukemia earlier after Cas-Br-M MuLV injection than control nontransgenic littermates. It is anticipated that retroviral infection of *Cnr2* transgenics will add to our insight into the cooperation between *Evi11*/*Cnr2*, the target gene in *Evi12*, and other proto-oncogenes. Nevertheless, the frequent coincidence of *Evi11*/*Cnr2* and *Evi12* in the Cas-Br-M MuLV-induced primary tumors suggests that the target genes in these two loci cooperate in leukemogenesis.

Evi12 is located upstream of the gene encoding the molecular chaperone *Tra1*/*Grp94*. The glucose-regulated stress protein Tra1/Grp94 is involved in protein processing and stimulates strong antitumor responses (41). *Tra1*/*Grp94* is ubiquitously expressed and the most abundant glycoprotein in the ER of eukaryotic cells (30). Tra1/Grp94 and another ER chaperone Grp78 are upregulated severalfold during differentiation of the macrophage cell line M1 after IL-6 stimulation (38) and *Grp94*/*Grp78* also induces resistance to apoptosis (26, 27, 31). These examples suggest that changes in *Tra1*/*Grp94* expression may affect normal differentiation or apoptosis of hematopoietic cells. Furthermore, expression of TRA1/GRP94 is elevated in human breast cancer cells (25a) and increased expression of *Tra1*/*Grp94* in a model of rat colon adenocarcinoma has been associated with greater tumorigenicity (32). This would imply that provirus in Evi12 should increase the expression of *Tra1*/*Grp94*. However, retroviral insertion in *Evi12* occurred outside the conserved regulatory elements that are responsible for basal expression as well as the inducibility of the *Tra1*/*Grp94* promoter (8, 29), and we could not demonstrate any significant changes in levels of *Tra1*/*Grp94* expression in cells containing proviral insertions in *Evi12*. Moreover, although it has recently been shown that *Tra1*/*Grp94* is tightly regulated by hematopoietic growth factors (6), no differences in the regulation of *Tra1*/*Grp94* expression after IL-3 starvation and IL-3 stimulation were observed in NFS107 compared to DA3 cells (data not shown). Thus, our results do not provide evidence to support the hypothesis that *Tra1*/*Grp94* represents the proto-oncogene affected by proviral insertion in the myeloid cell line NFS107 or the Cas-Br-M MuLV-induced primary tumors.

The proviruses in the Cas-Br-M MuLV-induced primary leukemias integrated in the opposite orientation compared to the direction of transcription of *Tra1*/*Grp94* (Fig. 6). This might suggest that not *Tra1*/*Grp94* but another gene downstream of the provirus insertions is the proviral target in *Evi12*. The transcriptional activation of this potential target gene may be by promoter insertion since proviruses integrated in a relatively small region of 1.7 kb (21, 55). To identify other potential proto-oncogenes in *Evi12*, an exon trapping system that we recently developed (51) is currently being applied to several bacterial artificial chromosome clones covering approximately 250 kb of the *Evi12* locus.

Since leukemic spleen and thymus contain normal tissue as well and the amount of normal tissue depends on the degree of tumor progression, frequent low intensity of the rearranged

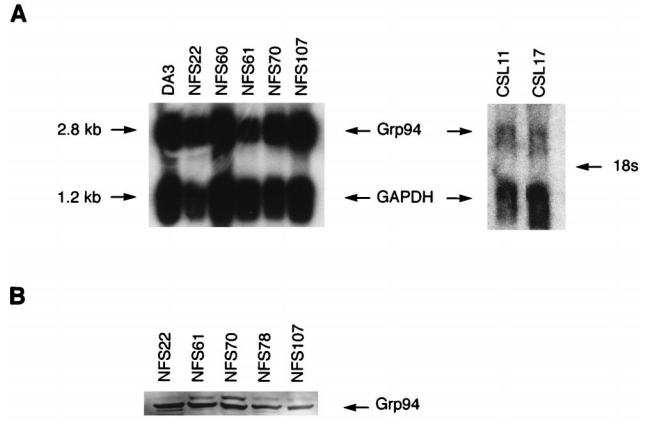

FIG. 6. Expression of *Tra1*/*Grp94* mRNA in NFS cell lines and primary tumors. (A) Northern blot analysis of MuLV-induced cell lines DA3, NFS22, NFS60, NFS61, NFS70, and NFS107 (*Evi12*) and primary tumors CSL11 (*Evi12*) and CSL17 (*Evi12*). Filters were hybridized with full-length cDNA of *Tra1*/*Grp94* (30) cloned from NFS22. (B) Western blot analysis of MuLV-induced cell lines NFS22, NFS61, NFS70, NFS78, and NFS107 (*Evi12*) with an anti-Grp94 antibody.

Evi11 and *Evi12* alleles in relation to the normal as well as variation between the primary tumors was shown by Southern blot analysis. Underrepresentation of the rearranged allele may be caused by polymorphism. However, since most of the proviral insertions have been cloned and sequenced and since Southern blot analysis of all tumors has been carried out with multiple restriction enzymes, the possibility of rearrangements as a result of polymorphism in the outbred NIH/Swiss mice is excluded.

In the cases of *Evi11* and *Evi12*, there is a strong selective advantage for integrations of MCF viruses. MCF viruses originate from recombination events between ecotropic MuLVs with endogenous proviruses involving the retroviral *env* gene and part of the LTR. Recombination results in the release of leukemogenic MCF viruses with an altered host range and the capability of superinfecting target cells. In a number of virus-induced hematologic diseases, particularly T-cell lymphomas, activation of the target proto-oncogene is regulated by insertion of viruses of the MCF type (4, 9). Provirus in *Evi11* contains a unique *Eco*RI site downstream of the 5′ LTR and is therefore distinct from the highly lymphomagenic NS-6(186) MCF virus, which has been cloned from a thymic T-cell lymphoma in NFS mice inoculated with Cas-Br-M MuLV (9). In *Evi12* the proviral genomes contain an altered *env* region characteristic for MCF viruses (44). Although, the exact role of MCF viruses is still unclear, the invariable insertion of MCF type proviruses and not Cas-Br-M MuLVs in *Evi11*/*Cnr2* and *Evi12* suggests an important role for MCF viruses in the activation of the target proto-oncogenes.

Evi11/*Cnr2* and *Evi12* retroviral insertions have been found in myeloid as well as in lymphocytic leukemias. Thus, there is no apparent correlation between morphology of the leukemia and proviral insertion in *Evi11*, *Evi12*, or both (Table 1). To define the phenotypes of *Evi11*/*Cnr2* and *Evi12* rearranged as well as nonrearranged leukemias more exactly, all primary tumors are currently being analyzed by fluorescence-activated cell sorter analysis with lymphoid- and myeloid-specific antibodies. The fact that *Evi11*/*Cnr2* and *Evi12* were identified in myeloid as well as in lymphoid lineages suggests that those insertions are early transforming events of immature multipotent progenitor cells. Other genetic defects may ultimately determine whether immature myeloid or lymphoid cells accumulate in the hematopoietic system.

Evi12 was mapped on mouse chromosome 10 by interspecific backcross analysis, and this mapping result was confirmed by the cytogenetic location of *Tra1*/*Grp94* (28). No putative proto-oncogenes have been identified in the mouse locus yet. *Evi12* is distinct from the known MuLV common integration sites *Mml1* (24) and *Mis2* (43), which both map close to *c-Myb* on mouse chromosome 10. *TRA1*/*GRP94* was cytogenetically mapped to human 12q24.2→24.3 (49). Subsequently, human *TRA1*/*GRP94* was placed on a yeast artificial chromosome contig representing 12q22–q23 (45). Thus, *EVI12* is located on human 12q22–24 as well. Although, no recurrent chromosomal breakpoints in human acute myeloid leukemia (AML) have been assigned to the human chromosomal region 12q22–24, an individual AML patient with a translocation between 3q21 and 12q24 has been described (56). Interestingly, 12q22 and 12q24 breakpoints have been associated with chronic lymphocytic leukemia (23) and B-cell non-Hodgkin lymphoma (57), respectively. Thus, the chromosomal region 12q22–24 may be involved in AML, chronic lymphocytic leukemia, or B-cell non-Hodgkin lymphoma. It will be of interest to investigate whether the *Evi12* locus also represents a nonrandom chromosomal breakpoint region of human malignancies.

ACKNOWLEDGMENTS

We thank Debbie Householder for excellent technical assistance, Karola van Rooyen for preparation of the figures, Kirsten van Lom for morphological analysis of the primary tumors, and Alister C. Ward for critical reading of the manuscript.

This work was supported by the Dutch Cancer Foundation Koningin Wilhelmina Fonds, the Netherlands Organisation for Scientific Research NWO, the Royal Dutch Academy of Sciences KNAW and the National Cancer Institute, DHHS, under contract with ABL.

REFERENCES

1. **Adams, J. M., and S. Cory.** 1992. Oncogene co-operation in leukaemogenesis. Cancer Surv. **15:**119–141.
2. **Ben-David, Y., E. B. Giddens, K. Letwin, and A. Bernstein.** 1991. Erythroleukemia induction by Friend murine leukemia virus: insertional activation of a new member of the ets gene family, Fli-1, closely linked to c-ets-1. Genes Dev. **5:**908–918.
3. **Berger, R., L. Theodor, J. Shoham, E. Gokkel, F. Brok-Simoni, K. B. Avraham, N. G. Copeland, N. A. Jenkins, G. Rechavi, and A. J. Simon.** 1996. The characterization and localization of the mouse thymopoietin/lamina-associated polypeptide 2 gene and its alternatively spliced products. Genome Res. **6:**361–370.
4. **Bergeron, D., L. Poliquin, J. Houde, B. Barbeau, and E. Rassart.** 1992. Analysis of proviruses integrated in Fli-1 and Evi-1 regions in Cas-Br-E MuLV-induced non-T-, non-B-cell leukemias. Virology **191:**661–669.
5. **Berns, A.** 1991. Tumorigenesis in transgenic mice: identification and characterization of synergizing oncogenes. J. Cell Biochem. **47:**130–135.
6. **Brewer, J. W., J. L. Cleveland, and L. M. Hendershot.** 1997. A pathway distinct from the mammalian unfolded protein response regulates expression of endoplasmic reticulum chaperones in non-stressed cells. EMBO J. **16:** 7207–7216.
7. **Buchberg, A. M., H. G. Bedigian, N. A. Jenkins, and N. G. Copeland.** 1990. Evi-2, a common integration site involved in murine myeloid leukemogenesis. Mol. Cell. Biol. **10:**4658–4666.
8. **Chang, S. C., A. E. Erwin, and A. S. Lee.** 1989. Glucose-regulated protein (GRP94 and GRP78) genes share common regulatory domains and are coordinately regulated by common *trans*-acting factors. Mol. Cell. Biol. **9:**2153–2162.
9. **Chattopadhyay, S. K., B. M. Baroudy, K. L. Holmes, T. N. Fredrickson, M. R. Lander, H. C. D. Morse, and J. W. Hartley.** 1989. Biologic and molecular genetic characteristics of a unique MCF virus that is highly leukemogenic in ecotropic virus-negative mice. Virology **168:**90–100.
10. **Copeland, N. G., and N. A. Jenkins.** 1991. Development and applications of a molecular genetic linkage map of the mouse genome. Trends Genet. **7:**113–118.
11. **Cuypers, H. T., G. C. Selten, M. Zijlstra, R. E. de Goede, C. J. Melief, and A. J. Berns.** 1986. Tumor progression in murine leukemia virus-induced T-cell lymphomas: monitoring clonal selections with viral and cellular probes. J. Virol. **60:**230–241.
12. **Dechert, U., M. Weber, M. Weber-Schaeuffelen, and E. Wollny.** 1989. Isolation and partial characterization of an 80,000-dalton protein kinase from the microvessels of the porcine brain. J. Neurochem. **53:**1268–1275.
13. **Dechert, U., P. Weber, B. Konig, C. Ortwein, I. Nilson, W. Linxweiler, E. Wollny, and H. G. Gassen.** 1994. A protein kinase isolated from porcine brain microvessels is similar to a class of heat-shock proteins. Eur. J. Biochem. **225:**805–809.
14. **Galiegue, S., S. Mary, J. Marchand, D. Dussossoy, D. Carriere, P. Carayon, M. Bouaboula, D. Shire, G. Le Fur, and P. Casellas.** 1995. Expression of central and peripheral cannabinoid receptors in human immune tissues and leukocyte subpopulations. Eur. J. Biochem. **232:**54–61.
15. **Hartley, J. W., and W. P. Rowe.** 1976. Naturally occurring murine leukemia viruses in wild mice: characterization of a new "amphotropic" class. J. Virol. **19:**19–25.
16. **Holmes, K. L., W. Y. Langdon, T. N. Fredrickson, R. L. Coffman, P. M. Hoffman, J. W. Hartley, and H. C. D. Morse.** 1986. Analysis of neoplasms induced by Cas-Br-M MuLV tumor extracts. J. Immunol. **137:**679–688.
17. **Holmes, K. L., E. Palaszynski, T. N. Fredrickson, H. C. D. Morse, and J. N. Ihle.** 1985. Correlation of cell-surface phenotype with the establishment of interleukin 3-dependent cell lines from wild-mouse murine leukemia virus-induced neoplasms. Proc. Natl. Acad. Sci. USA **82:**6687–6691.
18. **Hunter, T.** 1991. Cooperation between oncogenes. Cell **64:**249–270.
19. **Ihle, J. N., A. Rein, and R. Mural.** 1984. Immunological and virological mechanisms in retrovirus-induced murine leukemogenesis. Viral Oncol. **4:**95–137.
20. **Jenkins, N. A., N. G. Copeland, B. A. Taylor, and B. K. Lee.** 1982. Organization, distribution, and stability of endogenous ecotropic murine leukemia virus DNA sequences in chromosomes of *Mus musculus*. J. Virol. **43:**26–36.
21. **Jonkers, J., and A. Berns.** 1996. Retroviral insertional mutagenesis as a strategy to identify cancer genes. Biochim. Biophys. Acta **1287:**29–57.
22. **Jonkers, J., H. C. Korswagen, D. Acton, M. Breuer, and A. Berns.** 1997.

Activation of a novel proto-oncogene, Frat1, contributes to progression of mouse T-cell lymphomas. EMBO J. **16:**441–450.
23. **Juliusson, G., and M. Merup.** 1998. Cytogenetics in chronic lymphocytic leukemia. Semin. Oncol. **25:**19–26.
24. **Koller, R., M. Krall, B. Mock, J. Bies, V. Nazarov, and L. Wolff.** 1996. Mml1, a new common integration site in murine leukemia virus-induced promonocytic leukemias maps to mouse chromosome 10. Virology **224:**224–234.
25. **Langdon, W. Y., P. M. Hoffman, J. E. Silver, C. E. Buckler, J. W. Hartley, S. K. Ruscetti, and H. C. D. Morse.** 1983. Identification of a spleen focus-forming virus in erythroleukemic mice infected with a wild-mouse ecotropic murine leukemia virus. J. Virol. **46:**230–238.
25a. **Lee, A.** Unpublished results.
26. **Li, L. J., X. Li, A. Ferrario, N. Rucker, E. S. Liu, S. Wong, C. J. Gomer, and A. S. Lee.** 1992. Establishment of a Chinese hamster ovary cell line that expresses grp78 antisense transcripts and suppresses A23187 induction of both GRP78 and GRP94. J. Cell Physiol. **153:**575–582.
27. **Little, E., and A. S. Lee.** 1995. Generation of a mammalian cell line deficient in glucose-regulated protein stress induction through targeted ribozyme driven by a stress-inducible promoter. J. Biol. Chem. **270:**9526–9534.
28. **Maki, R. G., R. L. Eddy, Jr., M. Byers, T. B. Shows, and P. K. Srivastava.** 1993. Mapping of the genes for human endoplasmic reticular heat shock protein gp96/grp94. Somat. Cell Mol. Genet. **19:**73–81.
29. **Maki, R. G., L. J. Old, and P. K. Srivastava.** 1990. Human homologue of murine tumor rejection antigen gp96: 5′-regulatory and coding regions and relationship to stress-induced proteins. Proc. Natl. Acad. Sci. USA **87:**5658–5662.
30. **Mazzarella, R. A., and M. Green.** 1987. ERp99, an abundant, conserved glycoprotein of the endoplasmic reticulum, is homologous to the 90-kDa heat shock protein (hsp90) and the 94-kDa glucose regulated protein (GRP94). J. Biol. Chem. **262:**8875–8883.
31. **McCormick, T. S., K. S. McColl, and C. W. Distelhorst.** 1997. Mouse lymphoma cells destined to undergo apoptosis in response to thapsigargin treatment fail to generate a calcium-mediated grp78/grp94 stress response. J. Biol. Chem. **272:**6087–6092.
32. **Menoret, A., K. Meflah, and J. Le Pendu.** 1994. Expression of the 100-kDa glucose-regulated protein (GRP100/endoplasmin) is associated with tumorigenicity in a model of rat colon adenocarcinoma. Int. J. Cancer **56:**400–405.
33. **Miles, C., M. J. Sanchez, A. Sinclair, and E. Dzierzak.** 1997. Expression of the Ly-6E.1 (Sca-1) transgene in adult hematopoietic stem cells and the developing mouse embryo. Development **124:**537–547.
34. **Morishita, K., E. Parganas, C. L. William, M. H. Whittaker, H. Drabkin, J. Oval, R. Taetle, M. B. Valentine, and J. N. Ihle.** 1992. Activation of EVI1 gene expression in human acute myelogenous leukemias by translocations spanning 300-400 kilobases on chromosome band 3q26. Proc. Natl. Acad. Sci. USA **89:**3937–3941.
35. **Morishita, K., D. S. Parker, M. L. Mucenski, N. A. Jenkins, N. G. Copeland, and J. N. Ihle.** 1988. Retroviral activation of a novel gene encoding a zinc finger protein in IL-3-dependent myeloid leukemia cell lines. Cell **54:**831–840.
36. **Moskow, J. J., F. Bullrich, K. Huebner, I. O. Daar, and A. M. Buchberg.** 1995. Meis1, a PBX1-related homeobox gene involved in myeloid leukemia in BXH-2 mice. Mol. Cell. Biol. **15:**5434–5443.
37. **Munro, S., K. L. Thomas, and M. Abu-Shaar.** 1993. Molecular characterization of a peripheral receptor for cannabinoids. Nature **365:**61–65.
38. **Nakai, A., T. Kawatani, S. Ohi, H. Kawasaki, T. Yoshimori, Y. Tashiro, Y. Miyata, I. Yahara, M. Satoh, and K. Nagata.** 1995. Expression and phosphorylation of BiP/GRP78, a molecular chaperone in the endoplasmic reticulum, during the differentiation of a mouse myeloblastic cell line. Cell Struct. Funct. **20:**33–39.
39. **Nakamura, T., D. A. Largaespada, M. P. Lee, L. A. Johnson, K. Ohyashiki, K. Toyama, S. J. Chen, C. L. Willman, I. M. Chen, A. P. Feinberg, N. A. Jenkins, N. G. Copeland, and J. D. Shaughnessy, Jr.** 1996. Fusion of the nucleoporin gene NUP98 to HOXA9 by the chromosome translocation t(7;11)(p15;p15) in human myeloid leukaemia. Nat. Genet. **12:**154–158.
40. **Nakamura, T., D. A. Largaespada, J. D. Shaughnessy, Jr., N. A. Jenkins, and N. G. Copeland.** 1996. Cooperative activation of Hoxa and Pbx1-related genes in murine myeloid leukaemias. Nat. Genet. **12:**149–153.
41. **Nicchitta, C. V.** 1998. Biochemical, cell biological and immunological issues surrounding the endoplasmic reticulum chaperone GRP94/gp96. Curr. Opin. Immunol. **10:**103–109.
42. **Nichols, J., and S. D. Nimer.** 1992. Transcription factors, translocations, and leukemia. Blood **80:**2953–2963.
43. **Poirier, Y., C. Kozak, and P. Jolicoeur.** 1988. Identification of a common helper provirus integration site in Abelson murine leukemia virus-induced lymphoma DNA. J. Virol. **62:**3985–3992.
44. **Quint, W., W. Boelens, P. van Wezenbeek, T. Cuypers, E. R. Maandag, G. Selten, and A. Berns.** 1984. Generation of AKR mink cell focus-forming viruses: a conserved single-copy xenotrope-like provirus provides recombinant long terminal repeat sequences. J. Virol. **50:**432–438.
45. **Renault, B., J. Lieman, D. Ward, K. Krauter, and R. Kucherlapati.** 1995. Localization of the human achaete-scute homolog gene (ASCL1) distal to phenylalanine hydroxylase (PAH) and proximal to tumor rejection antigen (TRA1) on chromosome 12q22–q23. Genomics **30:**81–83.
46. **Sambrook, J., E. F. Fritsch, and T. Maniatis.** 1989. Molecular cloning: a laboratory manual, 2nd ed. Cold Spring Harbor Laboratory Press, Cold Spring Harbor, N.Y.
47. **Shannon, K. M., O. C. P., G. A. Martin, D. Paderanga, K. Olson, P. Dinndorf, and F. McCormick.** 1994. Loss of the normal NF1 allele from the bone marrow of children with type 1 neurofibromatosis and malignant myeloid disorders. N. Engl. J. Med. **330:**597–601.
48. **Srivastava, P. K., Y. T. Chen, and L. J. Old.** 1987. 5′-Structural analysis of genes encoding polymorphic antigens of chemically induced tumors. Proc. Natl. Acad. Sci. USA **84:**3807–3811.
49. **Srivastava, P. K., C. A. Kozak, and L. J. Old.** 1988. Chromosomal assignment of the gene encoding the mouse tumor rejection antigen gp96. Immunogenetics **28:**205–207.
50. **Valk, P., S. Verbakel, Y. Vankan, S. Hol, S. Mancham, R. Ploemacher, A. Mayen, B. Löwenberg, and R. Delwel.** 1997. Anandamide, a natural ligand for the peripheral cannabinoid receptor is a novel synergistic growth factor for hematopoietic cells. Blood **90:**1448–1457.
51. **Valk, P. J., S. Hol, Y. Vankan, J. N. Ihle, D. Askew, N. A. Jenkins, D. J. Gilbert, N. G. Copeland, N. J. de Both, B. Löwenberg, and R. Delwel.** 1997. The genes encoding the peripheral cannabinoid receptor and alpha-L-fucosidase are located near a newly identified common virus integration site, Evi11. J. Virol. **71:**6796–6804.
52. **Valk, P. J. M., M. Joosten, Y. Vankan, B. Löwenberg, and R. Delwel.** 1997. A rapid RT-PCR based method to isolate complementary DNA fragments flanking retrovirus integration sites. Nucleic Acids Res. **25:**4419–4421.
53. **Vogelstein, B., and K. W. Kinzler.** 1993. The multistep nature of cancer. Trends Genet. **9:**138–141.
54. **Wilkie, T. M., D. J. Gilbert, A. S. Olsen, X. N. Chen, T. T. Amatruda, J. R. Korenberg, B. J. Trask, P. de Jong, R. R. Reed, M. I. Simon, et al.** 1992. Evolution of the mammalian G protein alpha subunit multigene family. Nat. Genet. **1:**85–91.
55. **Wolff, L.** 1997. Contribution of oncogenes and tumor suppressor genes to myeloid leukemia. Biochim. Biophys. Acta **1332:**67–104.
56. **Yamagata, N., C. Shimazaki, T. Kikuta, H. Hirai, T. Sumikuma, Y. Sudo, E. Ashihara, H. Goto, T. Inaba, N. Fujita, and M. Nakagawa.** 1997. A translocation between 3q21 and 12q24 in a patient with minimally differentiated acute myeloid leukemia (AML-M0). Cancer Genet. Cytogenet. **97:**90–93.
57. **Zani, V. J., N. Asou, D. Jadayel, J. M. Heward, J. Shipley, E. Nacheva, K. Takasuki, D. Catovsky, and M. J. Dyer.** 1996. Molecular cloning of complex chromosomal translocation t(8;14;12)(q24.1;q32.3;q24.1) in a Burkitt lymphoma cell line defines a new gene (BCL7A) with homology to caldesmon. Blood **87:**3124–3134.